Biogeosciences Discuss., 8, 10823–10857, 2011
www.biogeosciences-discuss.net/8/10823/2011/
doi:10.5194/bgd-8-10823-2011

Biogeosciences Discussions

Discussion Paper | Discussion Paper | Discussion Paper | Discussion Paper |

Budget of N_2O emissions at the watershed scale: role of land cover and topography (the Orgeval basin, France)

G. Vilain, J. Garnier, P. Passy, M. Silvestre, and G. Billen

CNRS/UPMC, UMR7619 Sisyphe, 4 place Jussieu, 75005 Paris, France

Received: 19 October 2011 – Accepted: 23 October 2011 – Published: 8 November 2011

Correspondence to: G. Vilain (guillaume.vilain@upmc.fr)

Published by Copernicus Publications on behalf of the European Geosciences Union.

Abstract

Agricultural basins are the major source of N_2O emissions, with arable land accounting for half of the biogenic emissions worldwide. Moreover, N_2O emission strongly depends on the position of agricultural land in relation with topographical gradients, as footslope soils are often more prone to denitrification. The estimation of land surface area occupied by agricultural soils depends on the available spatial input information and resolution. Surface areas of grassland, forest and arable lands were estimated for the Orgeval sub-basin using two cover representations: the pan European CORINE Land Cover 2006 database (CLC 2006) and a combination of two databases produced by the Institut d'Aménagement et d'Urbanisme de la Région d'Île-de-France (IAU IDF), the MOS (Mode d'Occupation des Sols) combined with the Ecomos 2000, a land-use classification. In this study we have analyzed how different land-cover representations influence and introduce errors into the results of regional N_2O emissions inventories. A further introduction of the topography concept was used to better identify the critical zones for N_2O emissions, a crucial issue to better adapt the strategies of N_2O emissions mitigation. Overall, we observed that a refinement of the land-cover database led to a 5 % decrease in the estimation of N_2O emissions, while the integration of the topography decreased the estimation of N_2O emissions up to 25 %.

1 Introduction

Nitrous oxide (N_2O) is mainly produced by the microbial-mediated processes of nitrification and denitrification in soils. Its formation is influenced by several factors: climate (rainfall, temperature), soils (physical and chemical composition), substrate availability (nitrogen and carbon) as well as land management practices (Vilain et al., 2010; Skiba et al., 1998; Smith et al., 1998).

While the processes of N_2O production occur on a scale of less than one centimeter (i.e. the micro-scale or process scale), N_2O emissions are usually measured at scales of several centimeters to several hundred meters (Schimel and Potter, 1995). For example, a measurement at a single point (the point scale) could either be representative of emissions from a closed chamber with an area of 12 cm^2 or a micro-meteorological measurement of a 12-m^2 area, with the aim of obtaining results at the point scale that would reflect the micro-scale process and to extrapolate these measurements at the regional (possibly global) scale (Bouwman, 1996; Bouwman et al., 2002a,b).

However, the point scale can vary substantially (Folorunso and Rolston, 1984), because of the heterogeneity of denitrification activity or the presence of "hot spots" in soil (Ambus and Christensen, 1994; van den Heuvel et al., 2009). As a result, the N_2O fluxes emitted from soils at the observation scale show a high degree of spatial and temporal variability (Parton et al., 1988; Folorunso and Rolston, 1984) with coefficients of variation on the order of 500 % (Folorunso and Rolston, 1985). Therefore, the predictive relationships between N_2O fluxes and their associated control variables are very difficult to define (Corre et al., 1996).

A large number of simulation models have been developed to predict N_2O emissions, each one having its own philosophy and performance: STICS-NOE (Brisson et al., 2003; Hénault et al., 2005), DNDC (Li, 1996; Giltrap et al., 2010), CERES-EGC (Jones et al., 1986; Gabrielle et al., 2006b), NGAS (Parton et al., 1996, 2001) or DAYCENT (Parton et al., 1998; Del Grosso et al., 2001), and Image (Bouwman et al., 2006). The N_2O simulation models can be classified into three main categories: laboratory, field and regional/global levels.

Extrapolated data of N_2O emissions at the local (1–100 km) or regional (100–100 000 km) scale from point-scale measurements can be achieved using an intermediate scale, such as the plot (from 100–1000 m). A first source of error can be introduced by the scale and the accuracy of different land cover maps (Ellis, 2004; Bach et al., 2006; Schmit et al., 2006; Verburg et al., 2006). The high relation between land use and N_2O emissions highlights the importance of the land cover data when carrying out N_2O emissions inventories (Plant, 1999; Matthews et al., 2000).

BGD
8, 10823–10857, 2011

Evidencing the relationship with landscape makes it possible to partition the land into units defined by the relief (topographic attributes) and land use. A significant selection of sampling units (topography) may thus allow the extrapolation of flux measurements collected at points within these units (Corre et al., 1996).

This study aims to establish a nitrous oxide budget at a sub-basin scale of 100 km^2 (taking into account both direct and indirect emissions from groundwater and rivers). One of the objectives was to analyze how different land cover representations potentially introduce errors into the estimations of regional N_2O emissions inventories. A second major challenge was to assess the effect of topography on the estimation of the N_2O emissions at the basin scale. Accordingly, we then discussed agri-environmental measures that can decrease N_2O emissions as well as increase water quality.

2 Study site

The Orgeval basin belongs to the Seine basin (France) and is located approximately 70 km east of Paris. The whole study basin covers around 104 km^2. Annual rainfall is about 700 mm and the climate is semi-oceanic. The mean annual temperature is between 10 and 11 °C; the coldest month being January (mean temperature, 0.6 °C) and the warmest August (mean air temperature, 18 °C). The Orgeval watershed is particular in that it is highly homogenous in terms of pedology, climate and topography (mean altitude, 148 m, with few slopes except in the valleys).

Most of the Orgeval catchment surface is covered with a quaternary loess deposit (up to 10 m thick). The top layer comprises loess silt and the sublayer is enriched in clay, in winter producing a shallow water table and waterlogged soils due to its low permeability. Underneath the loess layer, two tertiary aquifer formations separated by discontinuous grey clay and a loamy gypsum layer interact with the streams (Mégnien, 1977). The shallowest formation is the Brie Limestone Oligocene formation, with a relatively short water residence time. The deepest formation is the Champigny Limestone Eocene, with a longer water residence time. The river incises all layers in its lower

BGD
8, 10823–10857, 2011

course and when the valley incises the impermeable green clay layer, springs located at the bottom of the Brie Limestone formation emerge and join the river. Most of the basin's surface area is artificially drained (about 90 % of the usable agricultural area) and dominated by agricultural land (82 %, i.e., 83 km^2); the remaining surface is covered by woods (17 % of the surface, i.e., 19 km^2) and urban zones or roads (1 % of the surface) (Fig. 1). Agriculture is dominated by grain crop rotation (with wheat, maize and barley) and field beans as the main rotation.

3 Material and methods

3.1 Determination of nitrification, denitrification and nitrous oxide production potentials in batch slurries

Emissions sources of nitrous oxide were assessed in laboratory experiments. Soils of the transect were placed in ideal optimal conditions for nitrification and denitrification to determine the maximum nitrification and denitrification rates as well as the nitrous oxide production by the two mechanisms and the ratio of (N_2O produced)/(nitrate reduced or produced) (see Garnier et al., 2010 for the methodology, results in Vilain et al., 2011; G. Vilain et al., unpublished data).

3.2 Water sampling

3.2.1 River

Dissolved N_2O concentrations in river water were monitored monthly in the Orgeval basin from January 2008 to December 2009. First- to third-order streams were sampled (see Fig. 2) and considered representative of all of the watershed's streams. Water samples from the river were directly taken in the riverbed in a 2-l bottle and transported to the laboratory for further analysis after storage at 4 °C. Water samples for N_2O were directly collected in 100-ml glass flasks, without air bubbles, fixed with

BGD
8, 10823–10857, 2011

$HgCl_2$ 6 % in order to stop any biological activity, and sealed with a rubber septum excluding any headspace gas.

3.2.2 Groundwater

Three piezometers were installed along a transect over an elevation gradient (mean slope, 2.2 %) from agricultural fields toward the stream including three slope positions (see Vilain et al., 2011 for full description): (i) plateau, (ii) midslope and (iii) river bank. The two piezometers in the plateau and midslope were inserted at a 15-m depth and reached the phreatic groundwater of the Brie. The piezometer situated in the River bank was inserted at a 3-m depth and reached the green clay layer. All were slotted on the bottom 1 m and wrapped with a 250-µm seamless polyester filter sock to prevent coarse sand particles from entering the well. Groundwater was sampled using an immerged pump from April 2008 to April 2010, with the piezometer emptied by flushing out water prior to collecting the sample in order to remove the standing water. Water samples were treated the same way as river samples.

3.3 Soil N_2O flux measurement

The nitrous oxide flux measurements were conducted weekly to bimonthly using the closed-chamber technique (Hutchinson and Livingston, 1993). This method, fully described in Vilain et al. (2010), consisted in measuring the gas fluxes from series of five aluminum non vented and hermetically closed chambers (open bases of 50 cm × 50 cm × 30 cm). Four gas samples were taken from each chamber headspace with a 30-ml Terumo® syringe and transferred to a 12.5-ml pre-evacuated glass vial (Labco Exetainer®) for transport to the laboratory. N_2O concentrations in gas samples were analysed in the laboratory using a gas chromatograph (Varian 3800) coupled with an electron capture detector (ECD). The gases were separated on a pre-column and a column packed with a Hayesep Q 80/100 mesh. Concentrations were calculated

BGD
8, 10823–10857, 2011

by comparing peak areas integrated with those obtained with standard N_2O concentrations (0.205, 0.540 and 3.30 ppm). N_2O fluxes were determined by calculating the linear regression slope of the N_2O concentration as a function of the sampling time (Livingston and Hutchinson, 1995) and adjusted for area and chamber volume. A sample set was accepted only when it yielded a statistically significant linear regression R^2 value according to the number of values taken into account.

Measurements (21 dates from May 2008 to August 2009) were taken on two agricultural plots chosen along a northwestward falling slope reaching the Avenelles River with an average inclination of 6 % in five topographical landscape positions from the shoulder to the footslope position. During this time period, plots were successively cropped to wheat/barley, an oat intercrop and corn.

3.4 Chemical measurements

3.4.1 Dissolved inorganic nitrogen

Ammonium was measured on filtered water (GF/F 0.4 µm porosity) with an autoanalyzer (Quaatro, Bran & Luebbe) using the indophenol blue method (Slawyk and MacIsaac, 1972). Nitrate was measured on filtered water, after cadmium reduction to NO_2^-, and NO_2^- was also automatically measured with the sulphanilamide method according to (Jones, 1984). Nitrite was also measured prior to cadmium reduction of NO_3^-.

3.4.2 Dissolved nitrous oxide

Nitrous oxide in water samples was determined with a gas chromatograph (Perichrom PR 2100) equipped with an electron capture detector (ECD). An aliquot (20 ml) of the water sample was degassed with an argon–methane (90/10) mixture, trapped and concentrated in a molecular sieve. After desorption, N_2O concentrations were determined in triplicate.

Discussion Paper | Discussion Paper | Discussion Paper | Discussion Paper |

BGD

8, 10823–10857, 2011

Budget of N_2O emissions at the watershed scale

G. Vilain et al.

3.5 Calculation of indirect emissions by rivers and aquifers

3.5.1 River

The N_2O flux across the water-atmosphere interface (F) can be calculated for each stream-order river of the Seine drainage network according to the relation:

$$F = K_{N_2O}([N_2O] - [N_2O]eq)$$

with F, ($\mu g\,N\,m^{-2}\,h^{-1}$) is the flux of N_2O from the water column to the atmosphere, $[N_2O]$, ($\mu g\,N\,l^{-1}$) is the mean N_2O concentration in river water, $[N_2O]eq$, ($\mu g\,N\,l^{-1}$) is the concentration at saturation for the atmospheric N_2O concentration K_{N_2O}, and ($m\,h^{-1}$) is the gas transfer velocity.

The saturation concentrations of N_2O in water at the present ambient atmospheric concentration (310 ppb) was determined using temperature-dependent values of N_2O solubility in water (Weiss and Price, 1980). This solubility can be expressed by the following polynomial relationship:

$$[N_2O]eq, (\mu g N l^{-1}) = 0.0002T^2 - 0.0167T + 0.5038$$

where T is the temperature in °C.

According to the work by Wanninkhof (1992) and Borges et al. (2004), the gas transfer velocity K_{N_2O} ($m\,h^{-1}$) in rivers, under conditions where the wind speed can be ignored, can be expressed as:

$$K_{N_2O} = 1.719\left[\left(600/Sc_{N_2O}\right)\cdot(v/d)\right]^{0.5}$$

with v ($m\,s^{-1}$) is the water flow rate, d (m) is the depth of the water column, Sc_{N_2O} is the Schmidt number, defined as the ratio between kinematic viscosity and mass diffusivity. It expresses the effect of temperature and the specificity of N_2O with respect to other gases on gas transfer properties. The Schmidt number for N_2O can be expressed as:

$$Sc_{N_2O} = 2056 - 137T + 4.317T^2 - 0.05435T^3$$

BGD
8, 10823–10857, 2011

Budget of N_2O emissions at the watershed scale

G. Vilain et al.

The morphological and hydrological characteristics of rivers of each stream order in the Seine river drainage network, under typical high-flow and low-flow conditions, are gathered in Table 1. The corresponding gas transfer velocities are calculated according to the above relationships.

3.5.2 Groundwater

Indirect emissions from groundwater can be estimated using hydrogeological data. We assumed that all the N_2O in the groundwater discharge is released into the atmosphere from agricultural drains or directly by diffusion from the water table to the unsaturated zone, and we used the estimated daily groundwater N_2O concentrations based on bi-monthly interval measures (considering a constant concentration rate beginning with the date of each sampling until the next sampling) and the daily water flow, for the Avenelles sub-basin (4570 ha). Then the N_2O flux emerging at springs can be estimated using the relation described by Verhoff et al. (1980):

$$\mathrm{Flx} = \frac{\Sigma C_\mathrm{i} Q_\mathrm{i}}{n \cdot a} \cdot 365$$

where Flx = N_2O flux, in $\mathrm{kg\,N\,ha^{-1}\,yr^{-1}}$, C_i = discrete instantaneous concentration ($\mathrm{kg\,N_2O\text{-}N\,l^{-1}}$), Q_i = corresponding instantaneous discharge ($\mathrm{l\,s^{-1}}$), n = study duration (days), and a = sub-basin area (ha).

3.6 Digital maps

3.6.1 Land use

The estimation of land-cover-based nitrous oxide emissions from the Orgeval basin is based on land use maps of the basin. Two databases with different resolutions were compared. The first one is the pan-European CORINE Land Cover 2006 database (CLC 2006) produced by the European Environmental Agency (EEA, 2007), which

BGD
8, 10823–10857, 2011

classifies lands into 44 classes. The minimum size of each polygon is 25 hectares. The database homogeneously covers the study area and using high-level aggregation classes (third level), the Orgeval basin is distributed into four CLC 2006 classes: arable land (class codes 211 and 242) with 79.08 %, forests (classes 311 and 324) with 19.57 %, grassland (class 231) with 0.76 % and urban areas (class 112) with 0.59 %. Giving the relatively small scale of the study area (104 km^2), the CLC 2006 database lacks precision and underestimates the area covered by grass and urban lands due to their fragmented nature (often less than 25 ha) (Fig. 1, left panel).

To correct this imprecision, a second database was used: it is a combination of two databases, both produced by the Institut d'Aménagement et d'Urbanisme de la Région d'Île-de-France (IAU IDF). The MOS (Mode d'Occupation des Sols) is a land-use classification in 81 classes covering the Île-de-France region with a geometric precision of 1/5000. (IAU, 2005a). The 25-m resolution raster, available free of charge on their website (http://www.iau-idf.fr/cartes/cartes-et-donnees-a-telecharger/donnees-a-telecharger.html), was used. It corresponds to the year 2003 and the classes are aggregated into 11 items. The MOS is mainly designed for urban planning; therefore seven out of the 11 classes detail urban land types and grasslands are aggregated with arable lands. This database was thus combined with the Ecomos 2000, a land use classification also produced by the IAU IDF and available on their website (IAU, 2005b). It details the "natural" classes from the MOS 1999 (forest and agricultural land) into 146 classes (distributed in six levels), excluding arable lands. The Ecomos maps 2000-m^2 polygons. The third level was used to extract forests and grasslands that were merged with the vectorized MOS data, thus dividing the "natural" classes into arable land, grassland and forest. For the Orgeval basin, this new combined land-use database (MOS + Ecomos) gives: 73.98 % arable lands, 19.50 % forests, 3.16 % grasslands, 3.15 % urban areas and 0.21 % water bodies (Fig. 1, right panel).

The use of MOS + Ecomos instead of CLC 2006 helps to accurately take grassland into account, reducing the part of cropland by almost 6 %.

BGD
8, 10823–10857, 2011

3.6.2 Topographic index

To extend the analysis even further, we developed an index to differentiate topographical landscape positions on cropland, as this was shown to largely influence the N_2O emissions (Vilain et al., 2010; van Kessel et al., 1993; Pennock et al., 1992; Izaurralde et al., 2004). The topographical index was first suggested as an indicator for surface runoff contributing areas by Kirkby (1975) and was the basis for the rainfall-runoff model called TOPMODEL (Beven and Kirkby, 1979). The most commonly used form of the index is defined as $\mathrm{Ln}(\alpha/\tan\beta)$, where α is the upslope contributing area to a given point of the catchment and β is a local surface slope angle (see Beven, 2001). This index represents the propensity of any point to become saturated. High topographic index values are good general indicators of wetlands (Curie et al., 2007; Merot et al., 2003). In this study, the topographic index was adapted into a Concentration Flux Position index (CFP index). Three topographic classes were defined according to the position within the landscape (Fig. 3). The topographic index map was calculated from a 25-m resolution digital elevation model produced by the Institut Géographique National (IGN) and is divided into three classes following the landscape segmentation approach proposed by Pennock et al. (1987):

i. The *footslope* class corresponds to areas where the topographic index is greater than the threshold value of 13 (see Curie et al., 2007). These areas with high topographic index values represent areas that are likely to be saturated. This class corresponds to the thalwegs and to areas located immediately at the foot of prominent reliefs such as buttes.

ii. The *slope class* was determined using the slope map. This class corresponds to the areas where the slope is greater than 2 %.

iii. The *shoulder class* corresponds to the areas where the slope is less than 2 % and the altitude higher than 100 m.

BGD
8, 10823–10857, 2011

3.6.3 Upscaling methods

Applying the three landscape position classes to the cropland class of the land-use databases (CLC 2006 and MOS + Ecomos) allowed us to upscale N_2O emissions to the Orgeval basin scale with two new approaches: Topography × CLC 2006 and Topography × (MOS + Ecomos).

4 Sources, emissions and transfer of nitrous oxide at the continuum scale

4.1 Nitrous oxide production by nitrification and denitrification in soils

Although the nitrate potential reduction and production rates by denitrification and nitrification, respectively, are on the same order of magnitude, a very significant difference occurs when regarding both the nitrous oxide production and the ratio of nitrous oxide produced by the two mechanisms (see Fig. 4). In order to determine the main mechanism responsible for the nitrous oxide concentrations in the groundwater, it is interesting to note that the ratio of N_2O produced by nitrification of 0.28 % is close to the mean ratio found in the plateau piezometer (0.26 %; see Vilain et al., 2011). On the other hand, regarding the seasonal peaks observed either after fertilization or heavy autumn rainfalls, they can be much higher and closer to the 45 % ratio found by denitrification. It can therefore be assumed that over a year nitrification is the main process occurring in soils, with the denitrification process occurring only during specific conditions such as fertilizer application associated with a higher soil moisture and hypoxia, conditions necessary for the denitrification process to take place (Bateman and Baggs, 2005; Davidson and Schimel, 1995; Linn and Doran, 1984).

4.2 Assessed gaseous N_2O fluxes from various land-use types

Measurements of N_2O emissions from a variety of land uses in agricultural, forest and grassland systems were taken in 2008 and 2009. Annual emission factors were then

BGD
8, 10823–10857, 2011

calculated as a function of land use (simple emission factors; see Table 2) and subclassified as a function of topography for the agricultural lands, following the landscape segmentation approach proposed by Pennock et al. (1987). The entire landscape was then divided into three segments (shoulder, slope and footslope) and the experimentally determined emission factors were assigned to each of these segments (see Table 2). This procedure highlights the importance of the difference in nitrous oxide emissions between the different topographic positions, with the highest emissions in low topographical positions (emission factor, 4.02 kg N_2O-N ha^{-1} yr^{-1}) with a decrease going up the slope (1.48 kg N_2O-N ha^{-1} yr^{-1} in the slope position and 1.06 kg N_2O-N ha^{-1} yr^{-1} in the shoulder position). For the other land uses (i.e. forest and grassland), we did not consider the influence of topography and applied the same emission factor regardless of topographic position, i.e. 0.55 and 0.69 kg N_2O-N ha^{-1} yr^{-1} for forest and grassland, respectively. When not considering the influence of topography for agricultural land, the simple mean emission factor used was 2.01 kg N_2O-N ha^{-1} yr^{-1} (from Vilain et al., 2010).

4.3 Indirect emissions

4.3.1 By groundwater: EF5g

According to the previously described calculation (see Sect. 3) and taking into account the N_2O concentrations from April 2008 to April 2010 in the plateau piezometer, the indirect N_2O flux from groundwater was estimated at 161.5 kg N_2O-N yr^{-1} for the entire Orgeval basin (Vilain et al., 2011).

4.3.2 By rivers: EF5r

The methodology proposed by Garnier et al. (2009) based on the determination of gas transfer velocities for all stream orders was followed. Then the observed supersaturation of dissolved N_2O concentrations in water of all stream orders were multiplied

BGD
8, 10823–10857, 2011

by the corresponding gas transfer rate and by the corresponding water surface area (Table 1), the result representing the indirect N_2O from drainage network emissions at the Orgeval basin scale (Fig. 3). Dissolved N_2O concentrations were higher in the first-order river (Mélarchez), ranging from 0.25 to 3.63 µg N_2O-N l^{-1} (mean, 1.27 µg N_2O-N l^{-1}) than in the second-order rivers (Avenelles) and third-order rivers (Theil), with concentrations ranging from 0.35 to 0.75 µg N_2O-N l^{-1} (mean, 0.50 µgN_2O-N l^{-1}) and from 0.37 to 1.46 µg N_2O-N l^{-1} (mean, 0.59 µg N_2O-N l^{-1}), respectively (Fig. 3). Temperature varied from 5 to 19 °C and the mean was 10 °C in winter and 15 °C in summer.

The calculated summer emissions were four times higher compared to winter emissions (1.67 kg N_2O-N ha^{-1} day^{-1} vs. 0.42 kg N_2O-N ha^{-1} day^{-1}, see Fig. 5). This trend confirms the findings of Garnier et al. (2009) at the larger scale of the entire Seine (75 000 km^2) for which summer emissions were twice as high as winter emissions. As also mentioned in Garnier et al. (2009), we observed a much higher contribution of small orders (here first order compared to second and third orders) to the global N_2O fluxes for water surfaces at the basin scale (91 % in summer and 71 % in winter).

Taking into account these calculated emission factors, the annual emission from the Orgeval basin drainage network can be estimated at 382 kg N_2O-N yr^{-1}.

5 Orgeval basin scale upscaling of N_2O emissions

Nitrous oxide emissions were calculated using the four different upscaling methods based on land-cover databases and topography (CLC 2006, MOS + Ecomos, Topo × CLC 2006, Topo × (MOS + Ecomos)). To each land use and topography class was applied the N_2O emission coefficients detailed in Table 2. Maps showing the predicted spatial distribution of nitrous oxide emissions rates in the Orgeval basin (expressed per surface area) under the four methods are presented in Fig. 6. Total annual N_2O emissions for the whole Orgeval basin are given in Table 3 by land-use class and for each upscaling method. Using the highest resolution database (MOS + Ecomos) reduces the N_2O emissions by more than 5 % compared to CLC 2006-based methods.

BGD
8, 10823–10857, 2011

When considering topography-based methods, the estimations were more than 20 % lower. By combining the added values of both approaches, e.g., a more precise land-cover database and topography classes, N_2O emissions estimations were lowered by almost 25 % (from 18.1 to 13.6 tons of N_2O-N a year for the whole Orgeval basin).

Table 4 presents the contribution of each landscape position class to the total budget. Both methods show that 50 % of the N_2O emissions in the Orgeval basin come from soils in the shoulder position, around 38 % from the footslope position and 12 % from the slope.

6 Discussion

6.1 Direct vs. indirect sources of N_2O

Nitrous oxide is produced in soil (and also to a lesser extent in aquifers and river sediments) by the two main mechanisms of nitrification and denitrification. Once produced in soil, N_2O can be either directly emitted to the atmosphere (direct emissions, Vilain et al., 2010) or stored in the soil pores and subsequently leached into the aquifer and then transported to the stream, leading to indirect emissions (Vilain et al., 2011; Garnier et al., 2009).

The novelty of this study is that it combines direct measurements of both direct and indirect N_2O emissions on the same agricultural sub-basin. Regarding the results of the estimations reported herein, it is clear that the total annual budget of N_2O emissions is driven by the direct emissions by soils, which account for 96 % of the total emissions (see Fig. 7). Indirect emissions by rivers and groundwater account for 3 and 1 %, respectively of the total emissions (Fig. 7).

6.2 Catchment nitrous oxide budget

At the basin scale, N_2O emissions were the highest in the footslope position on fertilized fields. The 11.4 % of the basin area occupied by this combination of land use

BGD
8, 10823–10857, 2011

and topographic class contributes 35.8 % of the annual N_2O emissions. The lowest emissions were found in forest zones, accounting for 19.5 % and the Orgeval basin and contributing 8.3 % of the annual emissions. On the whole, taking into account the finest direct N_2O estimations from soils (i.e., Topo × (Mos + EcoMos)) and the indirect emissions from groundwater and rivers, the N_2O budget for the whole Orgeval sub-basin can be estimated at 14.21×10^3 kg N_2O-N yr^{-1}.

This estimation, with regard to the sub-basin area, is equivalent to 1.33 kg N_2O-N ha^{-1} yr^{-1} considering both direct and indirect emissions and 1.28 kg N_2O-N ha^{-1} yr^{-1} considering only direct emissions, giving a proportion of 4 % for the indirect emissions. This estimation is well within the range of previous regional estimations in northern France, under similar climatic and pedologic conditions, from 0.84 to 2.0 kg N_2O-N ha^{-1} yr^{-1}, and slightly lower than our previous estimation of 2.0 kg N_2O-N ha^{-1} yr^{-1} for the whole Seine basin (Garnier et al., 2009). These experimental values are well within the range found with modelling approaches. The CERES-EGC biophysical soil-crop model coupled with the AROPAj economic model gave N_2O emissions in Picardie from 1.07 to 1.97 kg N_2O-N ha^{-1} yr^{-1} (Durandeau et al., 2010) while in the Ile-de-France region, again using the CERES-EGC model, Lehuger (2009) estimated N_2O emissions from 0.84 to 1.29 kg N_2O-N ha^{-1} yr^{-1}. Gabrielle et al. (2006b) used the same model run with geo-referenced input data on soils, weather and land use to map N_2O emissions from wheat-cropped soils and estimated N_2O emissions at 1.37 kg N_2O-N ha^{-1} yr^{-1}.

The nitrous oxide emissions at the regional level can be considered in two ways: as a magnitude of emissions or as a response of N fertilization applied. We have here considered only emissions, based on both topography and land use, even though the information on fertilizer use at the basin scale can be found and could improve this modelling exercise.

However, Freibauer (2003) modelled N_2O emissions at the European scale and showed a poor relationship between these emissions and fertilizer dose (0.4 %). The "fertilizer dose" factor seems to lose influence as the spatial area considered increases

BGD
8, 10823–10857, 2011

(Gabrielle et al., 2006a), confirmed by the study reported by Kaiser et al. (1998), which found a similar correlation coefficient of 0.6 %. Thus, not incorporating the fertilizer dose into our extrapolation may not have produced a significant error in the nitrous oxide flux estimation in the end.

One of the strengths of the methodology used herein is that it integrates the concept of topography into the estimation of N_2O emissions. Although this method can be refined, especially with regard to nitrogen rates applied on the field, this concept may be further used in subsequent coupling with process-based models such as STICS-NOE (Brisson et al., 2003; Hénault et al., 2005), DNDC (Li, 1996; Giltrap et al., 2010), CERES-EGC (Jones et al., 1986; Gabrielle et al., 2006b), NGAS (Parton et al., 1996, 2001) or DAYCENT (Parton et al., 1998; Del Grosso et al., 2001), for example.

6.3 Opportunities for nitrous oxide emissions mitigation

A promising direction for nitrous oxide emissions mitigation is the enlargement of buffer strip zones, particularly in low topographical positions. Schultz et al. (2009) reported that the riparian buffer zones have to be adjusted to fit the site. Indeed, all adjacent upland arable lands have different characteristics and then each one requires individual consideration in order to achieve the objectives in terms of nitrate reduction minimizing N_2O emissions. Landscape features can vary along the same water body such as presence or absence of wetlands, width of the floodplain, slope and soil type (Palone, 1998).

An additional alternative is to develop buffer strip biomass by harvesting (Spinelli et al., 2006). A conversion of buffer strip to biofuel products (such as switchgrass) can be a useful alternative (Isenhart et al., 2000; Lee et al., 2003). This could facilitate the expansion of buffer strips suggested above because it would reduce the loss of income by promoting the products of the riparian buffer zone.

In terms of ecological engineering, a conversion to agroforestry seems to be promising both in terms of nitrogen retention and removal, carbon sequestration, biodiversity conservation and soil enrichment (Jose, 2009; Montagnini and Nair, 2004). Moreover,

BGD
8, 10823–10857, 2011

employing agroforestry practices can provide food and fiber while maintaining habitats for threatened species and maintaining local biodiversity and associated ecosystem services such as pollination and pest control (Foley et al., 2005). Agroforestry systems such as riparian buffers have been proposed to control non-point source pollution coming from agricultural fields as they reduce the velocity of runoff by mechanisms such as infiltration, sediment deposition and nutrient retention (Jose, 2009). The effectiveness of these measures has been proved by several studies such as those reported by Udawatta et al. (2002), Anderson et al. (2009) and Lee et al. (2003), the latter showing a 20 % increase in nutrient retention in woody stem buffer compared to a switchgrass buffer. Trees with deep roots in agroforestry systems can even improve groundwater quality by taking up leached nutrient by tree roots. These nutrients are then recycled back into the system through root turnover and litterfall, increasing the nutrient use efficiency of the system (Van Noordwijk et al., 1996; Allen et al., 2004).

We tested an extreme hypothetical scenario where agriculture was excluded from the low topographical positions. For this purpose, we simply replaced the value of the emission coefficient corresponding to the agricultural footslope position (401.50 kg N_2O-N km^{-2} yr^{-1}) with the emission coefficient corresponding to grassland (69.35 kg N_2O-N km^{-2} yr^{-1}). Considering this scenario, with a 15.4 % loss of arable land, N_2O emissions of the whole watershed decreased by 29 % (i.e. 9620 vs. 13 666 kg N_2O-N yr^{-1}).

In conclusion, we have shown that the smoothness of the land-use data, as well as the integration of the topography are two important criteria for estimating N_2O emissions at the basin scale. A major challenge for precision conservation in greenhouse gas mitigation can be a variable rate application of N fertilizer in lower slope segments to ensure the highest possible fertilizer use efficiency and hence reduce N_2O emissions from these segments (Pennock, 2005).

Acknowledgements. This study was undertaken within the framework of the European AWARE programme, a project of the Seventh European Framework programme. The FIRE-FR3020 is also greatly acknowledged for its interdisciplinary research framework and for funding the site's equipment. We extend our thanks to the PIREN-Seine program for providing funding for the

BGD

8, 10823–10857, 2011

analysis. François Gilloots is sincerely acknowledged for having allowed us to conduct this research in his fields and for his willingness to contribute to scientific knowledge. Many thanks are due to the Cemagref (Patrick Ansart in particular for his help in the field). We also sincerely thank Benjamin Mercier and Olivier Tronquart for their kind laboratory and/or field assistance.

References

Allen, S., Jose, S., Nair, P., Brecke, B., Nkedi-Kizza, P., and Ramsey, C.: Safety net role of tree roots: experimental evidence from an alley cropping system, Forest Ecol. Manag., 192, 395–407, 2004.

Ambus, P. and Christensen, S.: Measurement of N_2O emission from a fertilized grassland: an analysis of spatial variability, J. Geophys. Res., 16, 549–555, doi:10.1029/94JD00267, 1994.

Anderson, S. H., Udawatta, R. P., Seobi, T., and Garrett, H. E.: Soil water content and infiltration in agroforestry buffer strips, Agroforest. Syst., 75, 5–16, 2009.

Bach, M., Breuer, L., Frede, H., Huisman, J., Otte, A., and Waldhardt, R.: Accuracy and congruency of three different digital land-use maps, Landscape Urban Plan., 78, 289–299, 2006.

Bateman, E. J. and Baggs, E. M.: Contributions of nitrification and denitrification to N_2O emissions from soils at different water-filled pore space, Biol. Fert. Soils 41, 379–388, 2005.

Beven, K. J.: Rainfall-runoff Modelling: The Primer, Wiley, Chichester, 2001.

Beven, K. J. and Kirkby, M. J.: A physically based, variable contributing area model of basin hydrology, Hydrol. Sci. Bull., 24, 43–69, 1979.

Bouwman, A. F.: Direct emission of nitrous oxide from agricultural soils, Nutr. Cycl. Agroecosys., 46, 53–70, 1996.

Bouwman, A. F., Boumans, L. J. M., and Batjes, N. H.: Emissions of N_2O and NO from fertilized fields: summary of available measurement data, Global Biogeochem. Cy., 16, 1058, , 2002a.

Bouwman, A., Boumans, L., and Batjes, N.: Modeling global annual N_2O and NO emissions from fertilized fields, Global Biogeochem. Cy., 16, 1080, doi:10.1029/2001GB001812, 2002b.

Bouwman, A., Kram, T., and Goldewijk, K. K.: Integrated modelling of global environmental change: an overview of Image 2.4, Netherlands Environmental Assessment Agency, Bilthoven, The Netherlands, 2006.

Brisson, N., Gary, C., Justes, E., Roche, R., Mary, B., Ripoche, D., Zimmer, D., Sierra, J.,

Bertuzzi, P., Burger, P., Bussière, F., Cabidoche, Y. M., Cellier, P., Debaeke, P., Gaudillère, J. P., Hénaul, C., Maraux, F., Seguin, B., and Sinoquet, H.: An overview of the crop model STICS, Eur. J. Agron., 18, 309–332, 2003.
Corre, M. D., van Kessel, C., and Pennock, D. J.: Landscape and seasonal patterns of nitrous oxide emissions in a semiarid region, Soil Sci. Soc. Am. J., 60, 1806–1815, 1996.
Curie, F., Gaillard, S., Ducharne, A., and Bendjoudi, H.: Geomorphological methods to characterise wetlands at the scale of the Seine watershed, Sci. Total Environ., 375, 59–68, 2007.
Davidson, E. A. and Schimel, J. P.: Microbial processes of production and consumption of nitric oxide, nitrous oxide and methane, in: Biogenic Trace Gases: Measuring Emissions from Soil and Water, Cambridge University Press, Cambridge, 327–357, 1995.
Del Grosso, S. J., Parton, W. J., Mosier, A. R., Hartman, M. D., Brenner, J., Ojima, D. S., and Schimel, D. S.: Simulated interaction of carbon dynamics and nitrogen trace gas fluxes using the DAYCENT model, in: Modeling Carbon and Nitrogen Dynamics for Soil Management, Lewis Publishers, Boca Raton, FL, USA, 303–332, 2001.
Durandeau, S., Gabrielle, B., Godard, C., Jayet, P. A., and Le Bas, C.: Coupling biophysical and micro-economic models to assess the effect of mitigation measures on greenhouse gas emissions from agriculture, Climatic Change, 98, 51–73, 2010.
EEA: CLC2006 technical guidelines, EEA Technical report No.17/2007, available at: http://www.eea.europa.eu/publications/technical_report_2007_17, 2007.
Ellis, E. C.: Long-term ecological changes in the densely populated rural landscapes of China, Geoph. Monog. Series, 153, 303–320, 2004.
Foley, J. A., DeFries, R., Asner, G. P., Barford, C., Bonan, G., Carpenter, S. R., Chapin, F. S., Coe, M. T., Daily, G. C., Gibbs, H. K., Helkowski, J. H., Holloway, T., Howard, E. A., Kucharik, C. J., Monfreda, C., Patz, J. A., Prentice, I. C., Ramankutty, N., and Snyder, P. K.: Global consequences of land use, Science, 309, 570–574, 2005.
Folorunso, O. A. and Rolston, D. E.: Spatial variability of field-measured denitrification gas fluxes, Soil Sci. Soc. Am. J., 48, 1213–1219, 1984.
Folorunso, O. A. and Rolston, D. E.: Spatial and spectral relationships between field-measured denitrification gas fluxes and soil properties, Soil Sci. Soc. Am. J., 49, 1087–1093, 1985.
Freibauer, A.: Regionalised inventory of biogenic greenhouse gas emissions from European agriculture, Eur. J. Agron., 19, 135–160, 2003.
Gabrielle, B., Laville, P., Duval, O., Nicoullaud, B., Germon, J. C., and Hénault, C.: Process-based modeling of nitrous oxide emissions from wheat-cropped soils at the sub-regional

BGD
8, 10823–10857, 2011

scale, Global Biogeochem. Cy., 20, GB4018, doi:10.1029/2006GB002686, 2006a.
Gabrielle, B., Laville, P., Hénault, C., Nicoullaud, B., and Germon, J. C.: Simulation of nitrous oxide emissions from wheat-cropped soils using CERES, Nutr. Cycl. Agroecosys., 74, 133–146, 2006b.
Garnier, J., Billen, G., Vilain, G., Martinez, A., Silvestre, M., Mounier, E., and Toche, F.: Nitrous oxide (N_2O) in the Seine river and basin: observations and budgets, Agr. Ecosyst. Environ., 133, 223–233, 2009.
Garnier, J. A., Mounier, E. M., Laverman, A. M., and Billen, G. F.: Potential denitrification and nitrous oxide production in the sediments of the Seine river drainage network (France), J. Environ. Qual., 39, 449–459, 2010.
Giltrap, D. L., Li, C., and Saggar, S.: DNDC: a process-based model of greenhouse gas fluxes from agricultural soils, Agr. Ecosyst. Environ., 136, 292–300, 2010.
Hénault, C., Bizouard, F., Laville, P., Gabrielle, B., Nicoullaud, B., Germon, J. C., and Cellier, P.: Predicting in situ soil N_2O emission using NOE algorithm and soil database, Glob. Change Biol., 11, 115–127, 2005.
Hutchinson, G. L. and Livingston, G. P.: Use of chamber systems to measure trace gas fluxes, in: Agricultural Ecosystem Effects on Trace Gases and Global Climate, edited by: Harper, L. A., American Society of Agronomy, Madison, WI, USA, 79–93, 1993.
IAU: Institut d'Aménagement et d'Urbanisme de la Région d'Ile-de-France, Les derniers résultats du MOS 2003, Note Rapide sur l'Environnement No. 387, Paris, 2005a.
IAU: Institut d'Aménagement et d'Urbanisme de la Région d'Ile-de-France, ECOMOS 2000 ou la cartographie détaillée des milieux naturels en Île-de-France, Note Rapide sur l'Environnement No. 388, Paris, 2005b.
Isenhart, T., Schultz, R., and Mickelson, S.: Multispecies riparian buffers trap sediment and nutrients during rainfall simulations J. Environ. Qual., 29, 1200–1205, 2000.
Izaurralde, R. C., Lemke, R. L., Goddard, T. W., McConkey, B., and Zhang, Z.: Nitrous oxide emissions from agricultural toposequences in Alberta and Saskatchewan, Soil Sci. Soc. Am. J., 68, 1285–1294, 2004.
Jones, M. N.: Nitrate reduction by shaking with cadmium: alternative to cadmium columns, Water Res., 18, 643–646, 1984.
Jones, C. A., Kiniry, J. R., and Dyke, P. T: CERES-N Maize: A simulation model of maize growth and development, Texas A&M University Press, College Station, Temple, TX, 1986.
Jose, S.: Agroforestry for ecosystem services and environmental benefits: an overview,

BGD
8, 10823–10857, 2011

Budget of N_2O emissions at the watershed scale

G. Vilain et al.

Agroforest. Syst., 76, 1–10, 2009.
Kaiser, E. A., Kohrs, K., Kücke, M., Schnug, E., Heinemeyer, O., and Munch, J. C.: Nitrous oxide release from arable soil: importance of N-fertilization, crops and temporal variation, Soil Biol. Biochem., 30, 1553–1563, 1998.
Kirkby, M. J.: Hydrograph modelling strategies, in: Processes in Physical and Human Geography, edited by: Peel, R., Chisholm, M., and Haggett, P., Heinemann, London, 69–90, 1975.
Lee, K., Isenhart, T., and Schultz, R.: Sediment and nutrient removal in an established multi-species riparian buffer, J. Soil Water Conserv., 58, 1, 1–8, 2003.
Lehuger, S.: Modelling greenhouse gas balance of agro-ecosystems in Europe. PhD thesis, l'Institut des Sciences et Industries du Vivant et de l'Environnement, AgroParisTech, Thiverval-Grignon, France, 2009.
Li, C.: The DNDC model, NATO ASI Ser. I, 38, 263–268, 1996.
Linn, D. M. and Doran, J. W.: Effect of water-filled pore space on carbon dioxide and nitrous oxide production in tilled and nontilled soils, Soil Sci. Soc. Am. J., 1267–1272, 1984.
Livingston, G. P. and Hutchinson, G. L.: Enclosure-based measurement of trace gas exchange: applications and sources of error, in: Biogenic Trace Gases: Measuring Emissions from Soil and Water, Blackwell Scientific Publications, Oxford, 14–51, 1995.
Matthews, R., Wassmann, R., Knox, J., and Buendia, L.: Using a crop/soil simulation model and GIS techniques to assess methane emissions from rice fields in Asia, IV. Upscaling to national levels, Nutr. Cycl. Agroecosys., 58, 201–217, 2000.
Mégnien, C.: Hydrogéologie du centre du Bassin de Paris: contribution à l'étude de quelques aquifères principaux, Principaux résultats scientifiques et techniques du Service géologique national, Paris, Bureau de Recherches Géologiques et Minières, 122 pp., 1979.
Merot, P., Squividant, H., Aurousseau, P., Hefting, M., Burt, T., Maitre, V., Kruk, M., Butturini, A., Thenail, C., and Viaud, V.: Testing a climato-topographic index for predicting wetlands distribution along an European climate gradient, Ecol. Model., 163, 51–71, 2003.
Montagnini, F. and Nair, P.: Carbon sequestration: an underexploited environmental benefit of agroforestry systems, Agroforest. Syst., 61, 281–295, 2004.
Palone, R. S.: Chesapeake Bay Riparian Handbook: A Guide for Establishing and Maintaining Riparian Forest Buffers, US Dept. of Agriculture, Forest Service, Radnor, PA, 1998.
Parton, W. J., Mosier, A. R., and Schimel, D. S.: Rates and pathways of nitrous oxide production in a shortgrass steppe, Biogeochemistry, 6, 45–58, 1988.
Parton, W. J., Mosier, A. R., Ojima, D. S., Valentine, D. W., Schimel, D. S., Weier, K., and

BGD
8, 10823–10857, 2011

Budget of N_2O emissions at the watershed scale

G. Vilain et al.

Kulmala, A. E.: Generalized model for N_2 and N_2O production from nitrification and denitrification, Global Biogeochem. Cy., 10, 401–412, 1996.
Parton, W. J., Hartman, M., Ojima, D., and Schimel, D.: DAYCENT and its land surface submodel: description and testing, Global Planet. Change, 19, 35–48, 1998.
Parton, W. J., Holland, E. A., Grosso, S. J. D., Hartman, M. D., Martin, R. E., Mosier, A. R., Ojima, D. S., and Schimel, D. S.: Generalized model for NO_x and N_2O emissions from soils, J. Geophys. Res., 106, 17403–17419, 2001.
Pennock, D. J.: Precision conservation for co-management of carbon and nitrogen on the Canadian prairies, J. Soil Water Conserv., 60, 396–401, 2005.
Pennock, D. J., Zebarth, B. J., and De Jong, E.: Landform classification and soil distribution in hummocky terrain, Saskatchewan, Canada, Geoderma, 40, 297–315, 1987.
Pennock, D. J., van Kessel, C., Farrell, R. E., and Sutherland, R. A.: Landscape-Scale Variations in Denitrification, Soil Sci. Soc. Am. J., 56, 770–776, 1992.
Plant, R.: Effects of land use on regional nitrous oxide emissions in the humid tropics of Costa Rica, Ph.D. Dissertation, Department of Environmental Sciences, Wageningen Agricultural University, Wageningen, The Netherlands, 1999.
Schimel, D. S. and Potter, C. S.: Process modelling and spatial extrapolation, in: Biogenic Trace Gases: Measuring Emissions from Soil and Water, edited by: Matson, P. A. and Harriss, R. C., Blackwell Science, Oxford, England, 358–384, 1995.
Schmit, C., Rounsevell, M., and La Jeunesse, I.: The limitations of spatial land use data in environmental analysis, Environ. Sci. Policy, 9, 174–188, 2006.
Schultz, R. C., Isenhart, T. M., Colletti, J. P., Simpkins, W. W., Udawatta, R. P., and Schultz, P. L.: Riparian and upland buffer practices, in: North American Agroforestry: An Integrated Science and Practice, 2nd edn., ASA, Madison, WI, 163–218, 2009.
Skiba, U. M., Sheppard, L. J., MacDonald, J., and Fowler, D.: Some key environmental variables controlling nitrous oxide emissions from agricultural and semi-natural soils in Scotland, Atmos. Environ., 32, 3311–3320, 1998.
Slawyk, G. and MacIsaac, J. J.: Comparison of two automated ammonium methods in a region of coastal upwelling, Deep-Sea Res., 19, 521–524, 1972.
Smith, K. A., Thomson, P. E., Clayton, H., McTaggart, I. P., and Conen, F.: Effects of temperature, water content and nitrogen fertilisation on emissions of nitrous oxide by soils, Atmos. Environ., 32, 3301–3309, 1998.
Spinelli, R., Nati, C., and Magagnotti, N.: Biomass harvesting from buffer strips in Italy: three

BGD
8, 10823–10857, 2011
Budget of N_2O emissions at the watershed scale
G. Vilain et al.

options compared, Agroforest. Syst., 68, 113–121, 2006.

Udawatta, R. P., Krstansky, J. J., Henderson, G. S., and Garrett, H. E.: Agroforestry practices, runoff, and nutrient loss: a paired watershed comparison, J. Environ. Qual., 31, 1214–1225, 2002.

van den Heuvel, R. N., Hefting, M. M., Tan, N. C. G., Jetten, M. S. M., and Verhoeven, J. T. A.: N_2O emission hotspots at different spatial scales and governing factors for small scale hotspots, Sci. Total Environ., 407, 2325–2332, 2009.

van Kessel, C., Pennock, D. J., and Farrell, R. E.: Seasonal variations in denitrification and nitrous oxide evolution at the landscape scale, Soil Sci. Soc. Am. J., 57, 988–995, 1993.

Van Noordwijk, M., Lawson, G., Soumare, A., Groot, J. J. R., and Hairiah, K.: Root distribution of trees and crops: competition and/or complimentarity, in: Tree-crop interactions. a physiological approach, edited by: Ong, C. K. and Huxley, P. A., CAB International, Wallingford, 319–364, 1996.

Verburg, P. H., van Bodegom, P. M., van der Gon, H. A. C. D., Bergsma, A., and van Breemen, N.: Upscaling regional emissions of greenhouse gases from rice cultivation: methods and sources of uncertainty, Plant Ecol., 182, 89–106, 2006.

Verhoff, F. H., Yaksich, S. M., and Melfi, D. A.: River nutrient and chemical transport estimation, J. Env. Eng. Div., 106, 591–608, 1980.

Vilain, G., Garnier, J., Tallec, G., and Cellier, P.: Effect of slope position and land use on nitrous oxide (N_2O) emissions (Seine Basin, France), Agr. Forest Meteorol., 150, 1192–1202, 2010.

Vilain, G., Garnier, J., Tallec, G., and Tournebize, J.: Indirect N_2O emissions from shallow groundwater in an agricultural catchment (Seine Basin, France), Biogeochemistry, doi:10.1007/s10533-011-9642-7, in press, 2011.

BGD

8, 10823–10857, 2011

Budget of N_2O emissions at the watershed scale

G. Vilain et al.

Table 1. Nitrous oxide fluxes at the water-air interface for the summer and the winter period for different stream orders of the Orgeval basin.

Order	Surface water area (km^2)	Summer flux ($mg\,N\,m^{-2}\,d^{-1}$)	Winter flux ($mg\,N\,m^{-2}\,d^{-1}$)
First	0.1709	8.91 ± 7.65	4.67 ± 2.76
Second	0.0654	1.17 ± 0.47	0.84 ± 0.50
Third	0.0171	1.03 ± 0.45	1.05 ± 0.94

Table 2. Nitrous oxide emission for the types of land use associated with their respective surface area in the basin and calculations from coefficients including topographic segmentation.

	Emission coefficient $kg\ N_2O\text{-}N\ km^{-2}\ yr^{-1}$	Land area km^2	Calculation from emission coefficient $kg\ N_2O\text{-}N\ yr^{-1}$
Mean Cropland	200.75	78.94	15,847.36
Shoulder	105.85	58.76	6219.76
Slope	147.83	8.00	1182.63
Footslope	401.50	12.18	4890.57
Forest	54.75	20.81	1139.35
Grassland	69.35	3.37	233.64

BGD
8, 10823–10857, 2011

Table 3. N_2O emission estimations for the Orgeval basin by main land use type and calculated by each upscaling method (in kg N_2O-N yr^{-1}). CLC: Corine Land Cover; MOS: Mode d'Occupation des Sols; Ecomos: land use classification produced by the IAU IDF.

	CLC 2006	MOS + Ecomos	Topo + CLC 2006	Topo + MOS + Ecomos
Arable	16 959.80	15 847.36	13 201.26	12 292.95
Forest	1144.41	1139.35	1144.41	1139.35
Grass	56.73	233.64	56.73	233.64
Total	18 161	17 220	14 402	13 666

BGD
8, 10823–10857, 2011

Table 4. Contribution of the three topographic classes to the total N_2O flux, given for the two upscaling methods based on topography and land use (in kg N_2O-N yr^{-1}).

	Topo × CLC 2006	Topo × (MOS + Ecomos)
Shoulder	7259.93	7023.78
Slope	1727.33	1540.48
Footslope	5415.13	5101.68
Total	14 402	13 666

BGD
8, 10823–10857, 2011

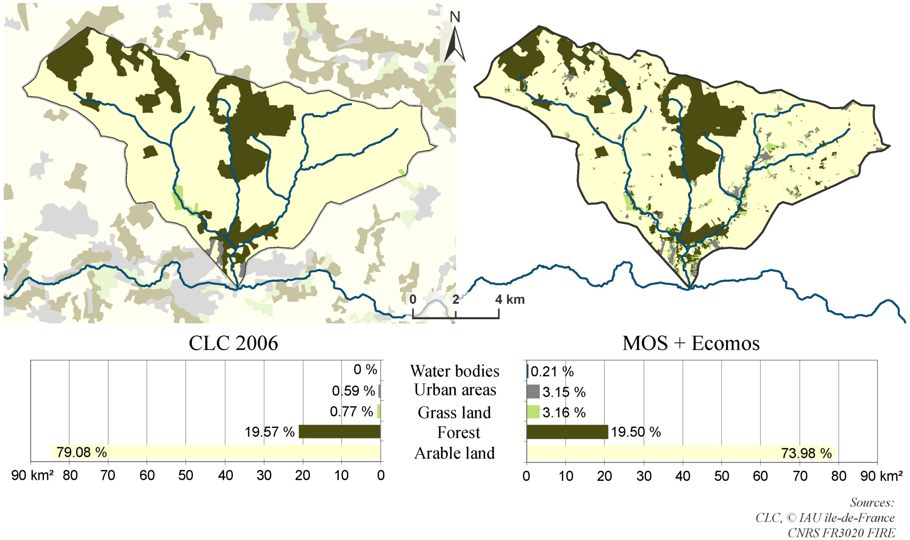

Fig. 1. Land use in the Orgeval basin in terms of forest, grassland and cropland. Urban areas are shaded grey. The drainage network is also indicated.

BGD
8, 10823–10857, 2011

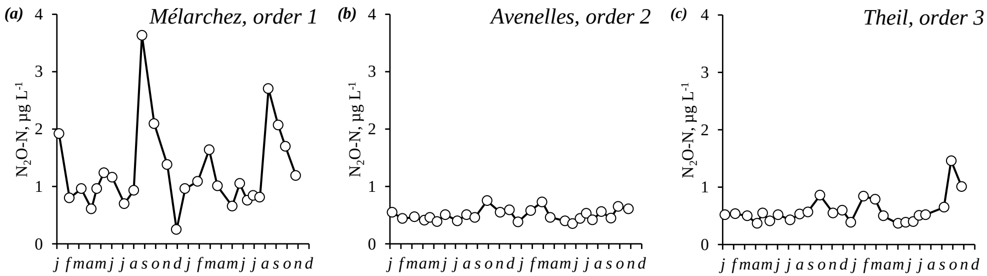

Fig. 2. Nitrous oxide concentrations between January 2007 and December 2008 in rivers at: **(a)** Mélarchez, first order; **(b)** Avenelles, second order and **(c)** Theil, third order.

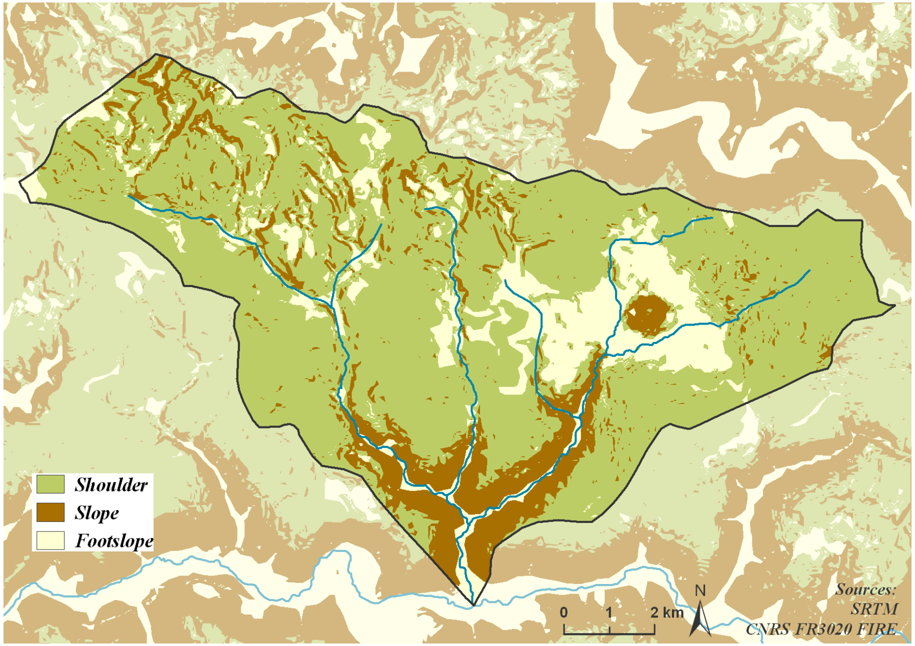

Fig. 3. Topographical map of the Orgeval basin.

BGD
8, 10823–10857, 2011

BGD
8, 10823–10857, 2011

Budget of N_2O emissions at the watershed scale

G. Vilain et al.

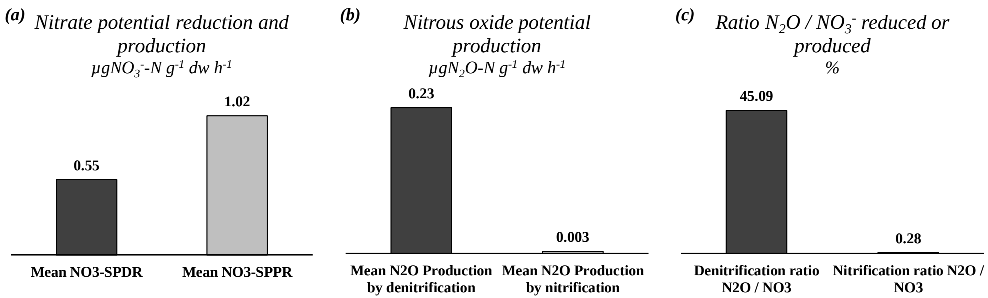

Fig. 4. Results of batch slurries: **(a)** potential nitrate reduction by denitrification and production by nitrification; **(b)** potential N_2O production and **(c)** ratio of N_2O production to nitrate reduced (denitrification) or produced (nitrification).

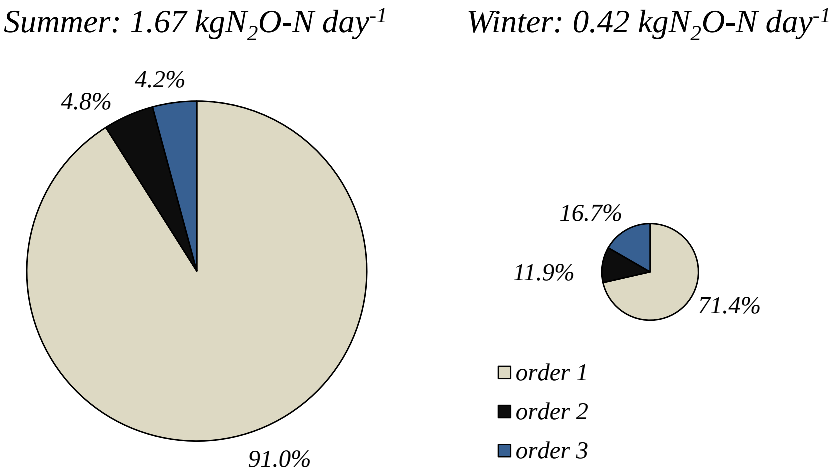

Fig. 5. Distribution of the daily N_2O emissions of the Orgeval drainage network, as a function of stream order for a winter and a summer period.

BGD
8, 10823–10857, 2011

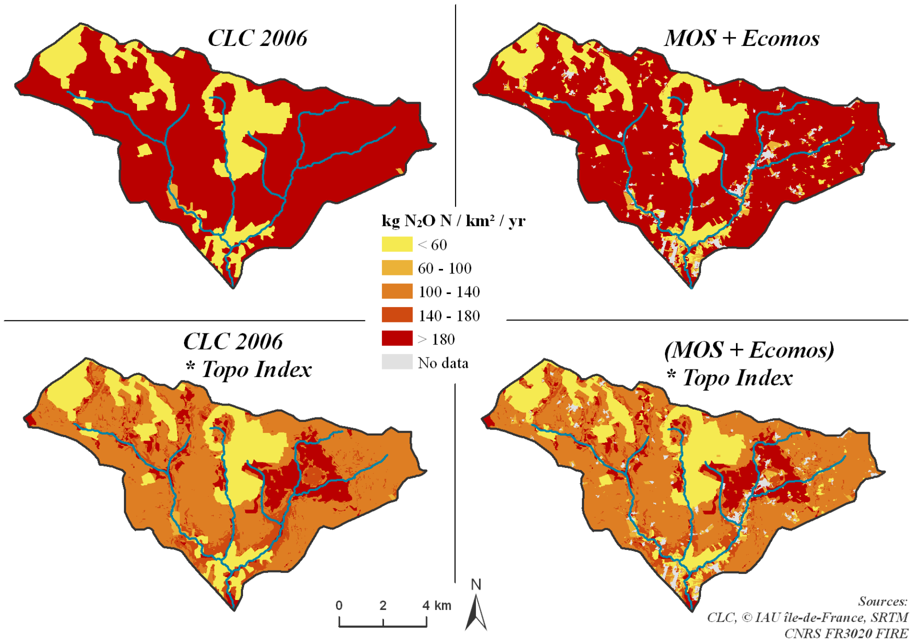

Fig. 6. Estimation of nitrous oxide emissions as a function of the land cover database and the topography.

BGD
8, 10823–10857, 2011

Budget of N_2O emissions at the watershed scale

G. Vilain et al.

Title Page
Abstract | Introduction
Conclusions | References
Tables | Figures
◀ | ▶
Back | Close
Full Screen / Esc
Printer-friendly Version
Interactive Discussion

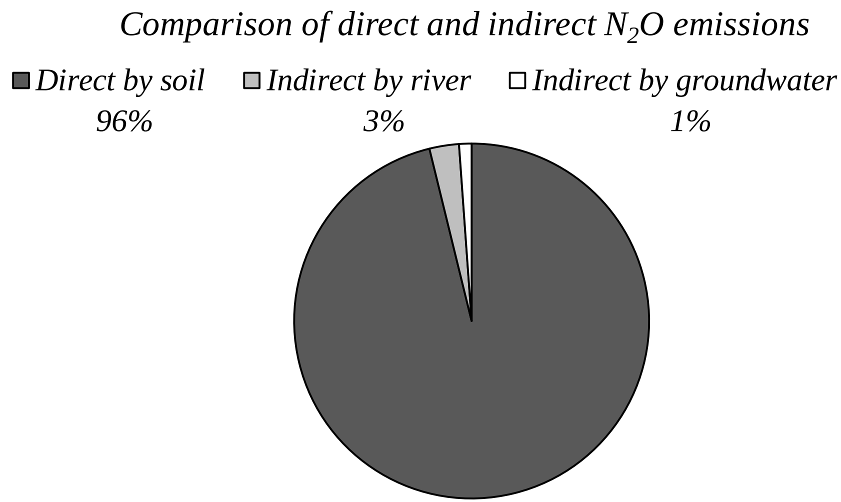

Fig. 7. Comparison of direct and indirect N_2O emissions at the Orgeval basin scale, based on the "Topo index × (MOS + Ecomos)" estimation.

BGD
8, 10823–10857, 2011